



NICA

NIGERIAN CORROSION ASSOCIATION

NICA/ICON/PAPR/92/8

PITTING AND CREVICE CORROSION SUSCEPTIBILITY OF SUPER AUSTENITIC STAINLESS STEELS IN SEA WATER

C.A. Loto, University of Lagos, Akoka, Lagos, Nigeria.

ABSTRACT

Pitting and crevice corrosion susceptibility of some super austenitic stainless steels in sea water were determined by field tests and laboratory examinations and analysis. This paper reports the observed corrosion susceptibility behaviour of the tubes' alloys. The inner surfaces of the steel tubes were exposed to flowing sea water a specially designed tests rig. The steam chamber part of the rig which was subjected to elevated temperature was the region where the middle portion of the tubes were located. After splitting in the laboratory, the tubes from the field test were examined with optical macro-/microscope (Wild M3C Model) and the scanning electron microscopy (S. E. M.). Analysis of the corrosion deposit was performed with the S. E. M. equipped with Energy Dispersive X-ray (EDAX) spectrometer, and the X-ray Diffraction spectroscopy (XRD). Though all the alloys, except the 316L, were found to be generally corrosion resistant, substantial crevice corrosion occurred under the strongly adherent calcareous layers deposited in the steam chamber portion of the tubes as observed in one of the runs made.

INTRODUCTION

The need to improve the length and predictability of service and to lessen the increasingly arduous task of conditions of heat exchanges in chemical industry such as the sulphuric acid manufacture and in condenser tubes at power plants cooled with sea water necessitated the present interest in the use of super austenitic stainless steels. These super austenitic stainless steels consist of high chromium (minimum of 20%); high molybdenum (minimum of 6%), nitrogen, silicon and in some cases copper. 316L alloy was used in this work for comparison purpose. Because of the high chloride concentration in sea water, the high service temperature, and biofouling among other factors, stainless steels are susceptible to pitting and crevice corrosion. Chromium and molybdenum of stainless steels have been recognised to strongly influence the resistance of stainless steels to localised corrosion.

There have been many literature reviews and several studies on pitting corrosion and the effect of alloying

elements on reducing it (1 - 10). It has been suggested that nitrogen in austenitic stainless steels is also an effective element to improve the resistance to pitting and crevice corrosion (5,6,7). Streicher (10) has also observed that the combined addition of molybdenum, nitrogen and silicon provided effective corrosion resistance behaviour to type 316 stainless steels.

It has been widely reported (11,12,13) that metal surfaces immersed in natural or industrial waters undergo a sequence of biological and inorganic changes that lead to biofouling and passivity respectively. Some of the ways in which biofilm may influence corrosion processes has been reported (14 -16).

In the super alloys under study, the effects of biofilms in sea water has not been much documented. However, further work on this is at present under investigation. In this work, corrosion resistance or behaviour of different types of super austenitic stainless steel alloys, in tubes, in which sea water was made to flow through, in a specially designed test rig located at HBOI, Florida, was studied by metallographic, electron-optic and spectroscopic methods. The work aims at making a significant contribution to the development of an understanding of the performance and service life of these super austenitic stainless steels in sea water environment.

EXPERIMENTAL METHODS

Field test

Nine tubes, each 2.14 metres long and 19 mm dia., made of different alloys of varying chemical composition, - Table 1, were used for the field test. A specially designed test rig located at the HBOI - Harbour Branch Oceanic Institution, Florida, was used for the test running. The tubes were specially fitted in the test rig in such a way as to permit uniform flow of sea water which was being pumped through. There was a steam chamber about 0.305 metres long located in about the middle portion of the tubes length and at which a predetermined steam temperature was maintained. Several test runs were made each lasting for 60 days averagely. New sets of tubes were used for

each test run. The water flow rate varied from one test run to another and it was predetermined. Table 2 gives a summary of the field test operating parameters. After each run, the tubes were brought to the laboratory after cutting to some specified lengths for further examination and analyses.

Laboratory examination and analyses.

The cut tubes were each split into two in the laboratory, with the weldment being at one part. The split tubes (already with biofouling) were then cleaned with water, detergent solution and hand brush. In some instances, photographs of the split tubes before and after cleaning were taken before further examination with the Wild M3C Model Optical macro/microscope. This microscope was used to observe the whole length surface of each tube to locate the occurrence or site of any pit or local corrosion attack sites.

Some of the microscopic corrosion pits' micrographs were taken with the Scanning electron microscopy (S. E. M.).

Biofilm/corrosion deposit composition analyses

Some of the cut ring samples, with the inner tube surface biofilms - specifically, the tubes made of 904L and 316L alloys from the steam chamber and the outlet portions, of two different test runs, were dried (dehydrated) in an oven at 100 °C for 4 hours after the distilled water and acetone cleaning. The specimens were each split into two and their surface biofilm composition analysed with the EDAX (Energy Dispersive X-ray) spectroscopy. The specimens used for the analysis were randomly selected. Further analysis was performed on the corrosion deposit, steam chamber's portion biofilm and the tube's outlet biofilm's composition using the x-ray Diffraction (XRD) technique and the EDAX. This was done on a selected tube, made of AL6XN alloy, that was used in two consecutive runs. This tube experienced variable operating parameters for a total of 120 days.

RESULTS

Visual, Metallographic and S. E. M. examinations

The biofilm on the inner surface of all the tubes, in general was slightly thick but easily removed with hand brush and water. The biofilm in the steam chamber portion was either very light, non-existent or with strong adherent calcareous deposit as observed in one of the test runs.

The super austenitic stainless steels were generally very corrosion resistant. The 316L used along with them was not corrosion resistant. It failed visibly in all the test runs. It was used for comparison purpose. All the other steel alloys corroded slightly with very little microscopic pits in the steam chamber and the steam outlet. Quite a number of microscopic pits or sites of

local corrosion attack were obtained along the weldment of the tubes made with AL6XN alloy in all the test runs. Most of the corrosion attack observed were not deep penetrating. They were shallow, flat, and somewhat roundish, figure 1.

The biofilm covering the inside surface of the tubes for one of the test runs was quite different. The striking difference was more noticeable in the steam chamber portions. The biofilm was very strongly adherent to the metal surface for all the tubes. Brush and soap solution could not remove this. If had to be scraped with the other metallic end of the brush used. Located under the adherent biofilm, were different forms of corrosion attack, mainly macroscopic, figure 2. A summary of this result is presented in figure 3. All the tubes had corrosion attack under the deposit but to varying degrees. Figures 4 - 7 are further indications of the corrosion attack on some of the tubes. The least corrosion attack occurred in the tubes made of 254 SMO (S31254) alloy followed by those made of 1925 HMO (NO8925) alloy. The corrosion attack concentrated mainly in the steam chamber portion.

EDAX spectroscopy analysis

The EDAX spectroscopy analysis results showed the presence of many chemical elements as presented, for example, in Figures 8-12. The biofilm collected from the steam chamber portion of the tube made of 904L (NO8904) alloy, figure 8, consists of Ca and P in addition to Fe, Cr and Ni. The tube's outlet biofilm appears to consist more of Fe, Si, and Cr. The steam chamber's portion biofilm of the tube made of 316L alloy, figure 9, consists of Si, Mg, P, Cl, and Ca among others. This tube's outlet biofilm consists more of Si, P, Al and Ca in descending order, figure 10. The corrosion deposit taken from a macroscopic pit in one of the tubes made of AL6XN (NO8367), consists relatively more proportion of Fe, Cr, Si and Ca. The presence of S and Mo is very difficult to ascertain as both share the same signal. The two elements would likely be present together. The tube's outlet portion biofilm consists more of Si, Cl, Ca and Fe in descending order. Ca was more predominant in the biofilm obtained from the steam chamber portion of the same tube. This was followed by the presence of Si, Mg, and Fe. The biofilm in the steam chamber was very adherent to the tube's inner surface.

X-ray diffraction analysis.

The results obtained from the x-ray diffraction analysis of the corrosion deposit from a pit located at the steam chamber's portion of one of the tubes made of AL6XN (NO8367) alloy, and the biofilm from the steam chamber and the outlet portions of the tube are presented in figures 11 - 13. The corrosion deposit consists of many phases of which the major ones are: Fe₂O₃, (Fe₃O₄) Fe(CrO₄) OH; and amorphous materials (substantial amount). Different phases were also present in the tube's steam chamber portion biofilm of which the major phases are:

Ca₃(SiO₃)₂ spinel - MgO amount of biofilm from NaCl as the small amount amorphous m

DISCUSSION
The over-all results are relatively testing conditions non-corrosive testing periods austenitic stainless not actually its relatively above, about alloys, does testing conditions with a situational layer deposits runs in this the steam chamber though to vary

In general, alloys tested very high at the Mo, Cr earlier mentioned known (i.e. corrosion rate) The high Mo have very However, magnitude be due, an metallurgical finishing & exemplified

The significant substantial steam chamber strong adherent was observed. Even some of the inconspicuous tested tubes the calcareous explain previous runs were condition unintentional strong, at the metal to unavailable inconsistent others due

$\text{Ca}_4(\text{SiO}_3)_3(\text{OH})_2$; calcite and aragonite - CaCO_3 ; spinel - MgO - like structure material and very small amount of biofilm and amorphous materials. The biofilm from the tube's outlet portion consists of: NaCl as the major crystalline material; CaCO_3 ; very small amounts of FeOOH ; and other crystalline and amorphous materials.

DISCUSSION

The over-all results obtained, suggest that all the alloys are relatively corrosion resistant under some particular testing conditions except the 316L which was generally non-corrosion resistant in sea water throughout the testing period. Though tested with other super austenitic stainless steels, 316L (S31603) alloy does not actually belong to this category of steels because of its relatively lower Mo content. The general statement above, about the relative corrosion resistance of the alloys, does not, however, hold under some particular testing condition(s). This assertion could be indicated with a situation whereby a strong adherent calcareous layer deposit occurred as observed in one of the test runs in this work. It led to under deposit corrosion in the steam chamber portion of all the steel tubes tested, though to varying degrees.

In general, the corrosion attack resistance of all the alloys tested, except the 316L, was attributable to the very high alloying contents of the steels - particularly the Mo, Cr, Ni, N and to some extent, Si and Mn. As earlier mentioned, these metallic elements have been known (1-9) as providing stable passivity for the corrosion resistance of these alloys in corroding media. The high Mo content, in particular, has been found to have very high stable passivating effect (1-4). However, the slight differences observed in the magnitude of their corrosion resistance capability, could be due, among others, to the influence of their variable metallurgical compositions and/or their surface finishing characteristics as presented in Table 1, and exemplified in figures 16 and 17.

The significant observation in this work is that substantial crevice corrosion attack occurred in the steam chamber portion of the tubes when there was strong adherent calcareous layer deposit. This situation was observed only once throughout the whole test runs made. Even when crevice condition was designed into some of the tubes, crevice corrosion attack occurred conspicuously at the longitudinal end of one of the tested tubes - 1925 HMO. The situation that has made the calcareous deposit possible is very difficult to explain precisely. This was because most of the test runs were carried out under similar operating conditions; though some with intentional and unintentional variations. An attempt to reproduce the strong, adherent and slightly thick calcareous deposit on the metals surface did not succeed. This might be due to unavoidable irregularity and anomaly of some inconsistent stoppages caused by power failures among others during the tests.

The tests were performed during different periods of the year. The seasonal variation could influence the amounts of dissolved ions-/chemicals in the sea water, especially the calcium carbonate and magnesium carbonate/sulphate species⁽¹⁷⁾. These situations could account, in part, for the difference obtained from one test run to another.

The problem created by the operating anomaly (such as stoppages) in the steam operating conditions could affect the non-uniformity of results; particularly with respect to calcareous deposition. The test rig operating conditions, with its elevated temperature at the steam chamber portion of the tubes could disturb the balance between the calcium compounds and CO_2 in the sea water used. This type of situation has been known to promote abnormal deposition of calcium carbonate on metal surfaces⁽¹⁸⁾. The strong adherence to the metal surface could be due to the high wall temperature. The high steam operating temperature would cause further precipitation of the CaCO_3 , MgCO_3 , and $\text{Mg}(\text{OH})_2$ etc. in the sea water flowing through the steam chamber⁽¹⁹⁾. Their solubility decreases with increasing temperature.

Deposition of calcareous layers is very much caused and enhanced by increase in pH of the sea water⁽²⁰⁻²⁴⁾. The high steam temperature did not only disturb the calcium compounds and CO_2 balance of the sea water, but also caused oxygen depletion within the steam chamber. The latter phenomenon would not only cause less passivity to the steel alloys but also increase the sea water alkalinity - and pH, with the consequential calcareous deposition which were mainly calcite and aragonite as confirmed by the x-ray diffraction analysis. Bacteria were not detected at the steam chamber section of any of the tubes where under-deposit corrosion attack occurred, and could not therefore be considered here.

The condition under the calcareous layer would be that of severe oxygen depletion and increased alkalinity - pH at the metal - electrolyte (sea water) interface. This in combination with the high chloride ions from the sea water, and the carbonate and sulphate ions, would cause the depassivation of the tube's metal passive film. As a result, anodic and cathodic corrosion sites were created leading to anodic and cathodic corrosion reaction. Crevice corrosion then occurred by the metal's anodic dissolution under the deposits. The corrosion reaction kinetics was definitely aided by the elevated temperature used.

Mechanistically, the over-all corrosion process must be that of synergism among the various factors involved; and crevice condition(s) must be available before any reasonable corrosion attack (crevice) could occur.

The EDAX spectroscopy analysis, (figures 8 -10), confirm the tubes' surface biofilm enrichment at the different areas of the tubes as consisting of different chemical elements. These include Ca, Mg, Cl, P, and

Si. The particular effect of these chemical elements on the biofilm structure, corrosion characteristics biofilm properties and hence on the corrosion of the tube metal alloys is not very clear. However, while chloride ions (Cl^-) would make a significant contribution towards the depassivation of the alloys' protective film, others such as Cr, Ni, Mo, Mg and Si were presumably giving some beneficial effects of stabilising the alloys protective film; while at the same time preventing the biofilm's growth that could lead to increased corrosion among other adverse effects.

The x-ray diffraction analysis confirms that the biofilm in the steam chamber was more enriched with Fe, Ca, and Mg than the outlet biofilm. It further confirmed the presence of $CaCO_3$ - calcite and aragonite, as the major composition of the calcareous layer deposited on the metal's surface which provided suitable crevice condition for corrosion attack.

CONCLUSION

1. All the super austenitic stainless steels gave general impressive corrosion resistance in sea water depending on the test conditions.
2. The 316L alloy, albeit not super stainless steel, was susceptible to pitting and crevice corrosion attack in sea water under all the testing conditions but more at elevated temperature(s) in the steam chamber.
3. All the alloys were susceptible to crevice corrosion attack but at varying degrees. Any condition that could create crevice environment during the use of these super austenitic stainless steels (in sea water) must be avoided.
4. Alloys 254 SMO (S31254) and 1925 HMO (NO8925) showed superior corrosion resistance relatively.
5. The role of the chemical elements and compounds within the biofilm matrix is not yet very clear, but some such as Cr, Ni, Mg, Mo, and Si, seem to contribute to stabilising the protective passive films on the metal alloys surface. Others such as $CaCO_3$, $MgCO_3$ - sulphates and hydroxide form the major constituent of the calcareous deposition and created crevice condition(s) on the metal surface for crevice corrosion attack. Calcareous deposition is definitely not good for these alloys in sea water.

ACKNOWLEDGEMENTS

This work was supported by grants from Chemetrics International Company Ltd; The University Research Incentive Fund (Province of Ontario), and the Natural Sciences and Engineering Research Council of Canada. The work was done at the Corrosion laboratory,

McMaster University, Hamilton, Ontario, in collaboration with Prof. M. B. Ives.

REFERENCES

1. A. J. Sedriks, "Corrosion of stainless steels", Wiley Intersci 1979 pp. 70 - 74.
2. Z. Skzlarska-Amialowska, "Pitting Corrosion of Metals", NACE, 1986, pp. 145-156.
3. T. P. Hoar, *J. Electroch. Soc* 117, p.170, (1970).
4. J. R. Ambrose, *Corrosion*, 34, P.27, (1977).
5. J. E. Truman, M. J. Coleman, K. R. Pirt, *Brit. Corr. J.* 12, 236, (1977).
6. J. Eckenrod, C. W. Kovack, ASTM STP 679, pp.17, (Philadelphia, PA, 1977),
7. K. Osozawa, N. Okato, in "Passivity and its Breakdown on Iron and Iron Based Alloys", NACE, Houston, TX 1976, pp.155.
8. R. Bandy D. Van Rooyen, *Corrosion*, 39, 227, (1983).
9. A. J. Sedriks, *Intl. Metal. Reviewa* 28, 306, (1983).
10. M. A. Streicher, *J. Electrochem. Soc.* 103, 375 (19567).
11. W. G. Characklis, *Biotech. Bioeng.* 23, 1923 - 1960, (1981).
12. J. W. Costerton, G. G. Geesey and K. J. Cheng, *Sci. Amer.* 238, 86-95, (1978).
13. H. A. Videla, in "Structure and Function of Biofilms" eds. W. G. Characklis and P. A. Wilderer, Chichester, U. K. (John Wiley & Sons Ltd). pp. 361-320, 1989a.
14. G. J. Brankevich, M. L. F. de Mele and H. A. Videla, *MTS J.*, 24, 3, pp. 8, (1990).
15. W. G. Characklis, B. J. Little and M. S. McCaughey, 'Biofilms and their effect on local chemistry, EPRI Workshop on Microbial Induced Corrosion, Charlotte, North Carolina, pp. 47, (1988).
16. W. G. Characklis and K. E. Cooksey, *Advances in Applied Microbiology*, 29, 93-138, (1983).
17. R. H. Heidersbach (Chairman), "Marine Corrosion", *Metals Handbook*, pp.894, ASM International (1987). Ninth edition.
18. F. L. Laque, *Marine Corrosion*, pp. 95-112, John Wiley & Sons, (1975).

19.

20.

21.

TA

CH

Tu

Nc

1

2&

3&

4&

8

9

TA

TE

19. S-H. Lin and S. C. Dexter, *Corrosion J.*, 44, 9, Sept., pp. 615-622, (1988).
20. K. G. Compton, Proc. Int. Corr. Forum, Toronto, 1975, NACE, Paper 13.
21. R. A. Humble, *Corrosion J.*, 4, 7, pp.358-370, (1948).
22. E. J. Zeller and J. L. Wray, *Bull. Amer. Assoc. Petro. Geog.*, 40, 1, pp.140-152.
23. S. L. Wolfson and W. H. Hart, *Corrosion J.*, 37, 2, pp. 70 - 76, (1981).
24. P. O. Gartland, E. Bardal, R. E. Andresen and R. Johnsen, *Corr. J.*, 40, 3, pp.127-133, (1984).

TABLE 1

CHEMICAL COMPOSITION OF SUPER AUSTENITIC STAINLESS STEELS

Tube NO	Alloy/UNS	ELEMENT %									
		Cr	Ni	Mo	Cu	Mn	C	P	S	Si	N
1	904L(N08904)	19.0-23	25.0	4.5	1.5	2.0	0.02	.045	.035	1.0	-
2&5	254SMO(S31254)	19.5-20.5	18.0	6.25	1.0	1.0	0.02	0.03	.01	.80	.20
3&7	AL6XN(N08367)	20.0-22	24.5	6.5	-	2.0	0.03	0.04	.03	1.0	.23
4&6	1925HMO(N08925)	24.0-26	20.0	6.5	1.0	1.0	0.02	0.045	.03	0.5	0.20
8	316L(S31603)	16-18	10-14	2-3	-	2.0	0.05	0.045	.03	1.0	-
9	Dummy	(Any of the above - as specified).									

TABLE 2

TEST CONDITIONS

Run #	Days	Steam Temp. (°C)	Water flow rate (ft/s)
4	59	140-160	4.5
5	64	162	4.5
6	61	160	9
7	60	130	1
8	61	160	9

LIST AND LEGENDS FOR THE FIGURES

FIGS

LEGENDS

1. S. E. M. micrograph of local corrosion attack on the inner surface of 1925HMO (NO8925) alloy tube.
2. Optical macrograph of under deposit corrosion on the inner surface of some of the split tested tubes. (1925 HMO alloy)
3. Schematic diagrams showing the locations and extent of corrosion in all the tested tubes (except the dummy) in one of the test runs where there was adherent calcareous deposit.
4. Optical microscope (Wild M3C Model) photograph of an under deposit local corrosion attack site in 904L alloy tube. Mag. x 10. (Glass ball size = 2.5mm).
5. Optical microscope photograph of an under deposit local corrosion attack site in AL6XN (NO8367) alloy tube. mag. x 6.4. (Glass ball size = 2.5mm).
6. Optical microscope photograph of other numerous under deposit local corrosion attack sites in AL6XN (NO8367) alloy tube. Mag. x 6.4 (Glass ball size = 2.5mm).
7. Optical microscope photograph of an under deposit local corrosion attack site in AL6XN (NO8367) alloy tube. Mag. x 6.4. (Glass ball size = 2.5mm).
8. FDAX analysis of the biofilm in the steam chamber portion of 904L (NO8904) alloy tube.
9. EDAX analysis of the biofilm in the steam chamber portion of 316L (S31603) alloy tube.
10. EDAX analysis of the biofilm in the outlet portion of 316L (S31603) alloy tube.
11. X-ray diffraction (XRD) spectroscopy analysis of the corrosion deposit from a macroscopic local corrosion attack site in the steam chamber portion of AL6XN (NO8367) alloy tube used as dummy in two test runs.
12. X-ray diffraction spectroscopy (XRD) analysis of the biofilm from the steam chamber portion of AL6XN (NO8367) alloy tube used as dummy in two runs.
13. X-ray diffraction spectroscopy (XRD) analysis of the biofilm obtained from the outlet portion of AL6XN (NO8367) alloy tube used as dummy in two test runs.

Fi

it
57)
=
am
am
n
of
al
mon
of
fwo

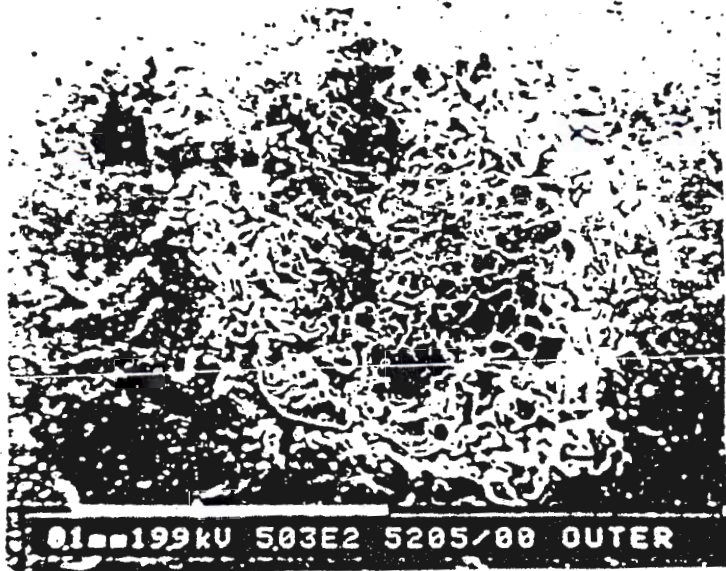


Fig. 1.

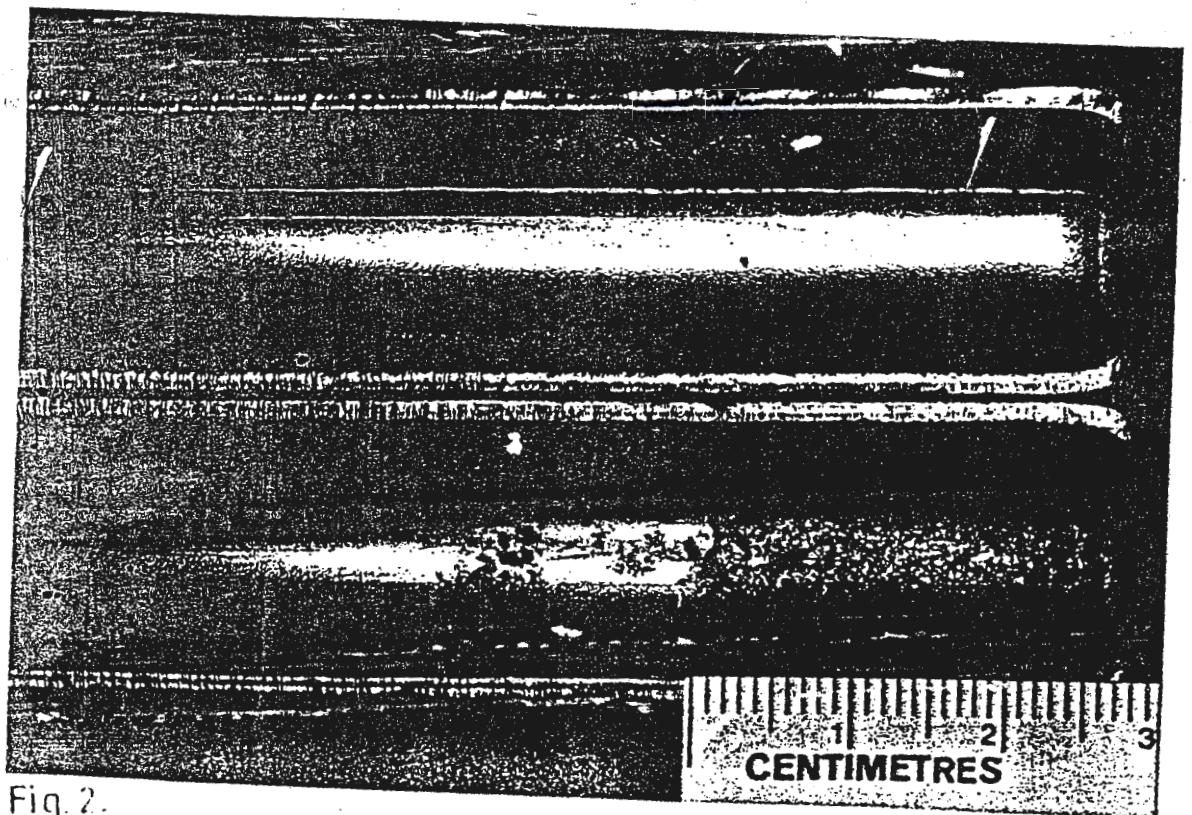


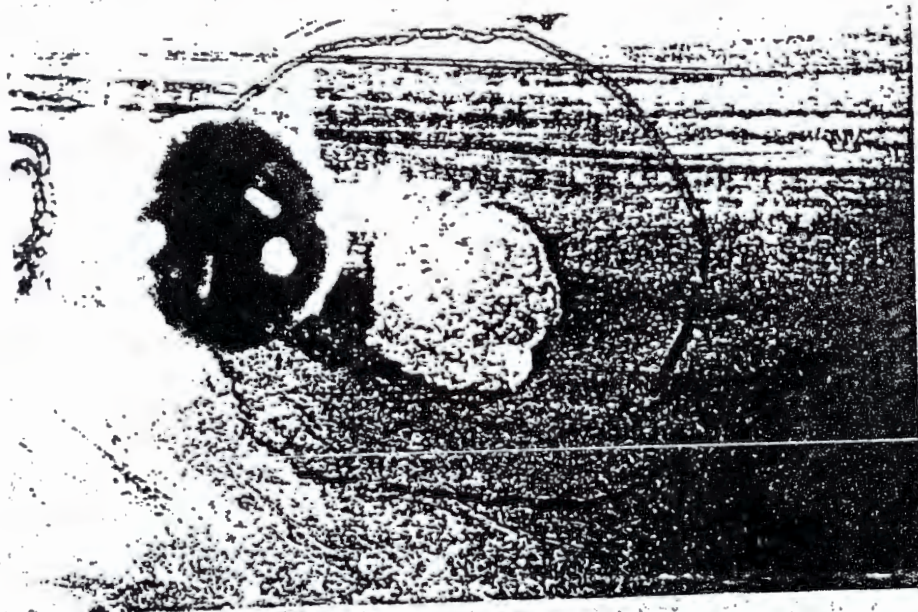
Fig. 2.

		Inlet	Steam	Outlet	
8	316L				
1	904L				
3	AL6				
7	AL6				
2	254				
5	254				
4	1925				
6	1925				
		A A'B'	B C	D E	F

Run 6 Tube Metallography

Fig. 5.

Fig. 3.



Fig

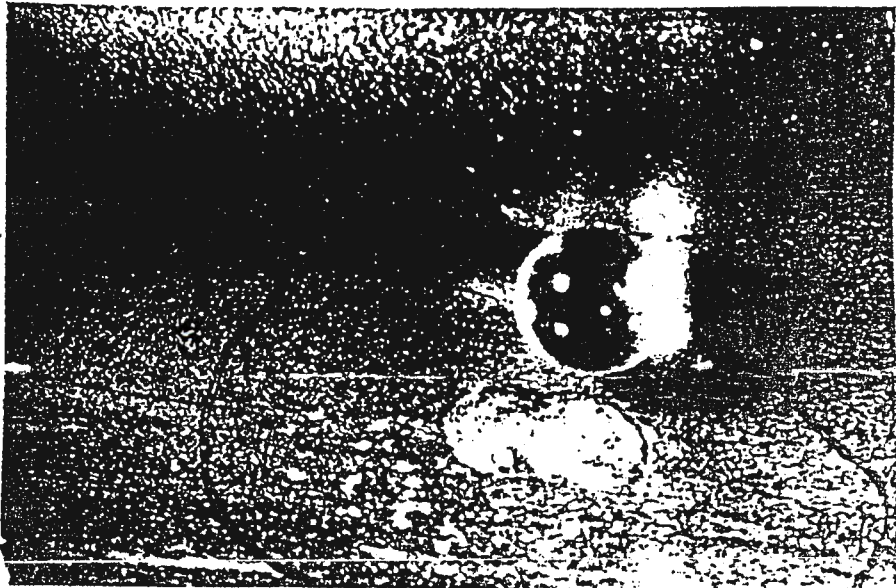


Fig. 5.



Fig. 6.



Fig. 7

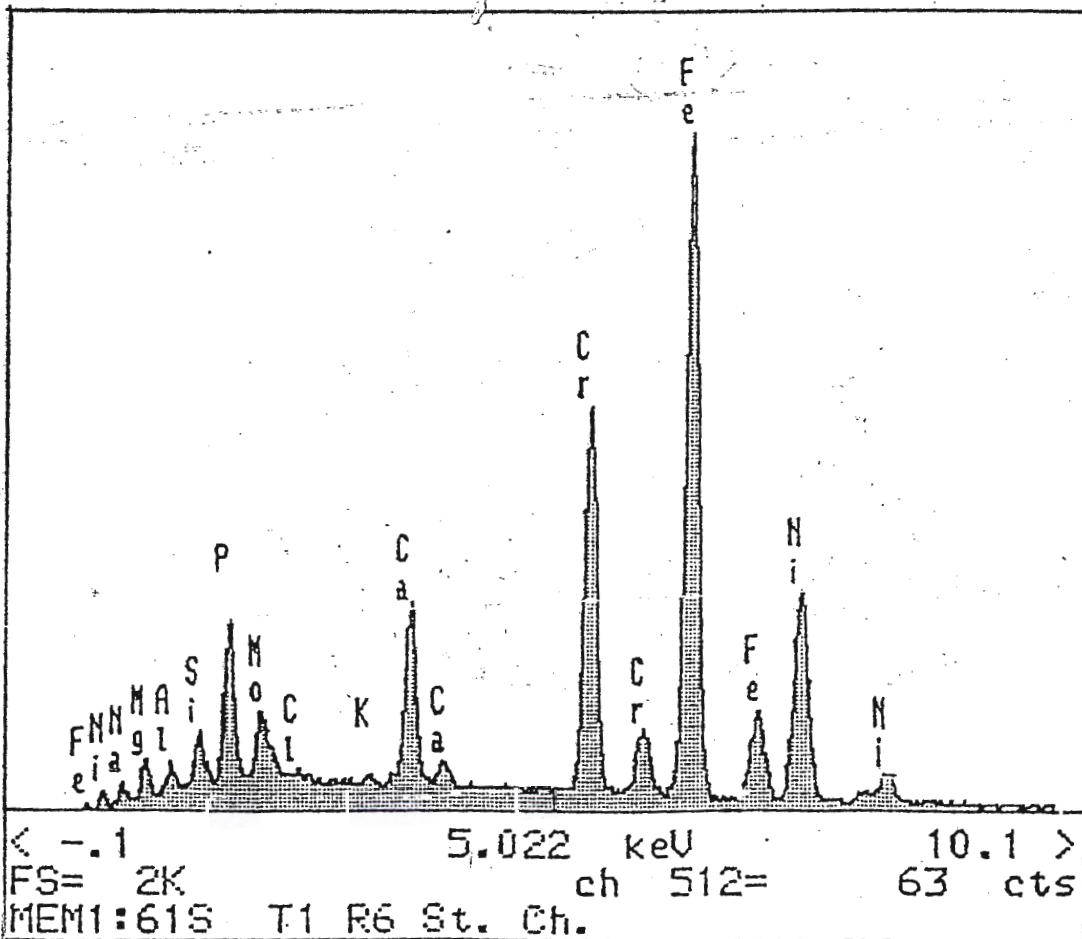


Fig. 8

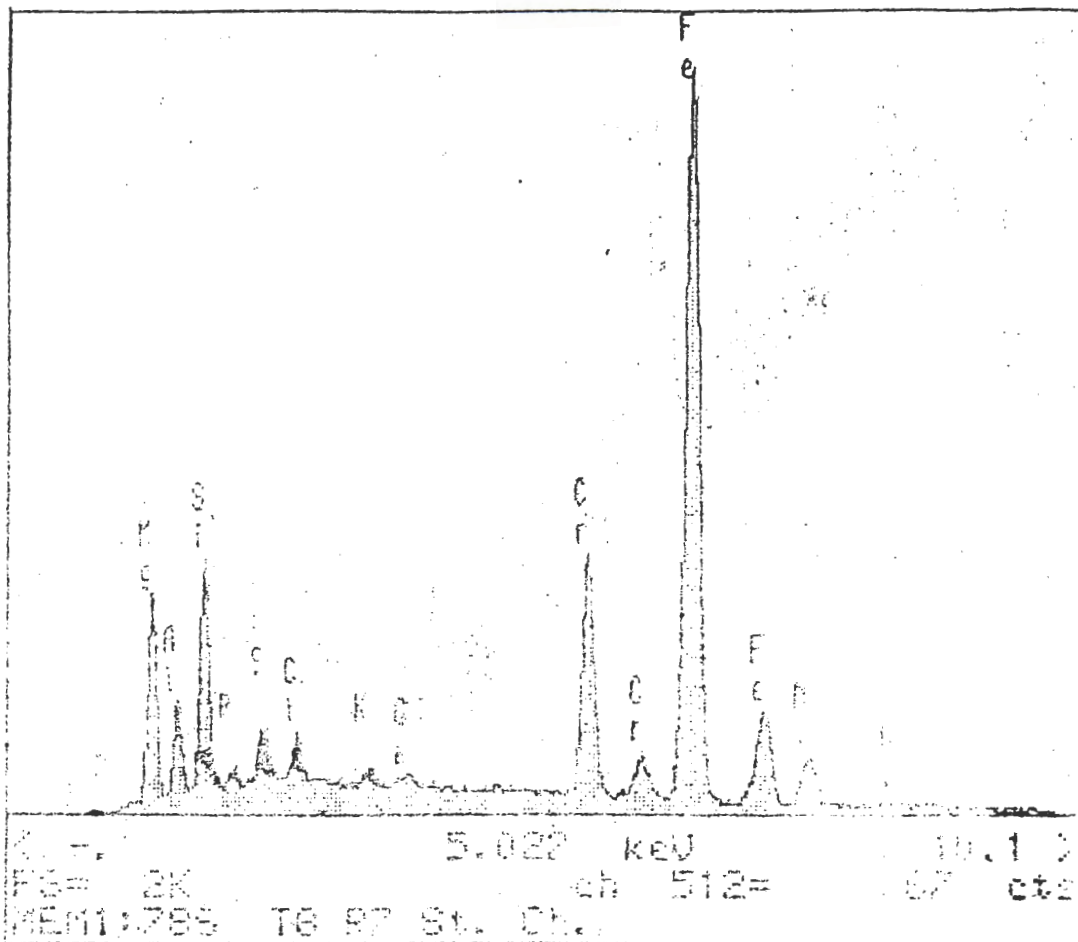
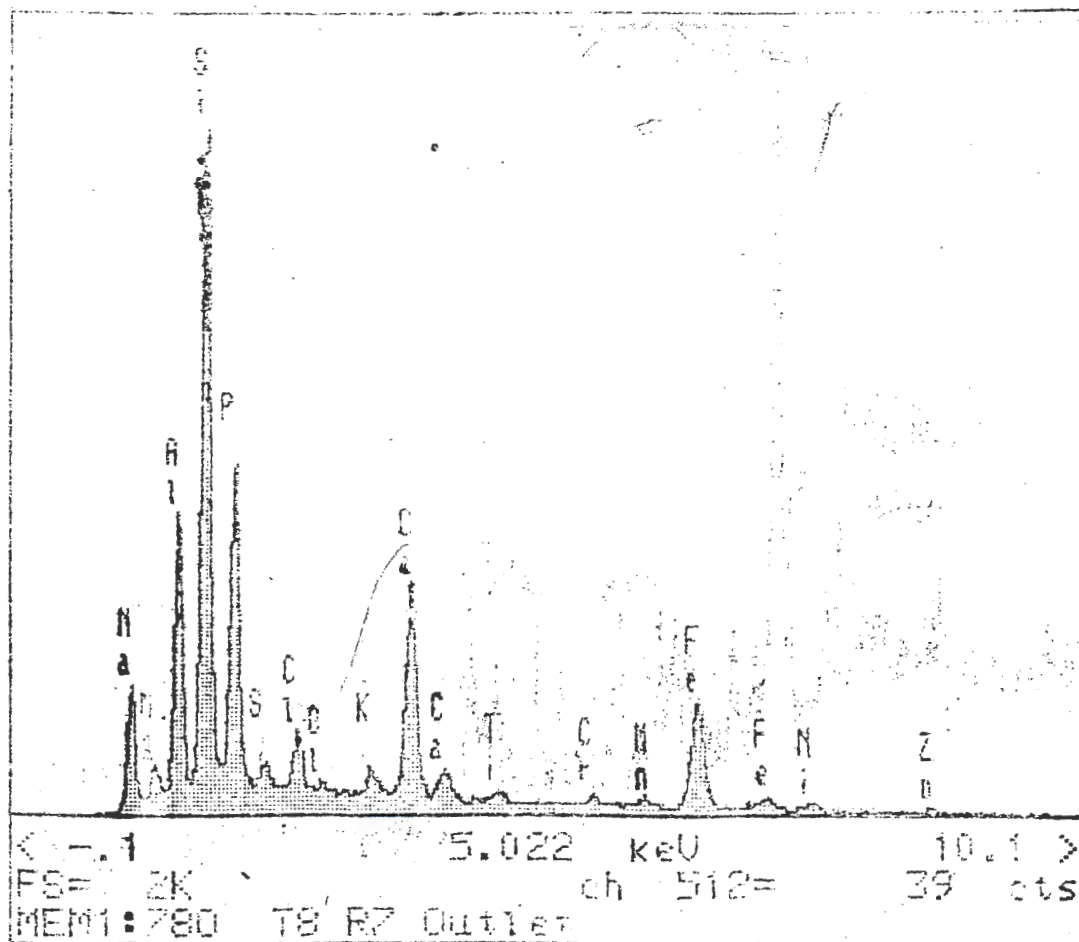


Fig. 5



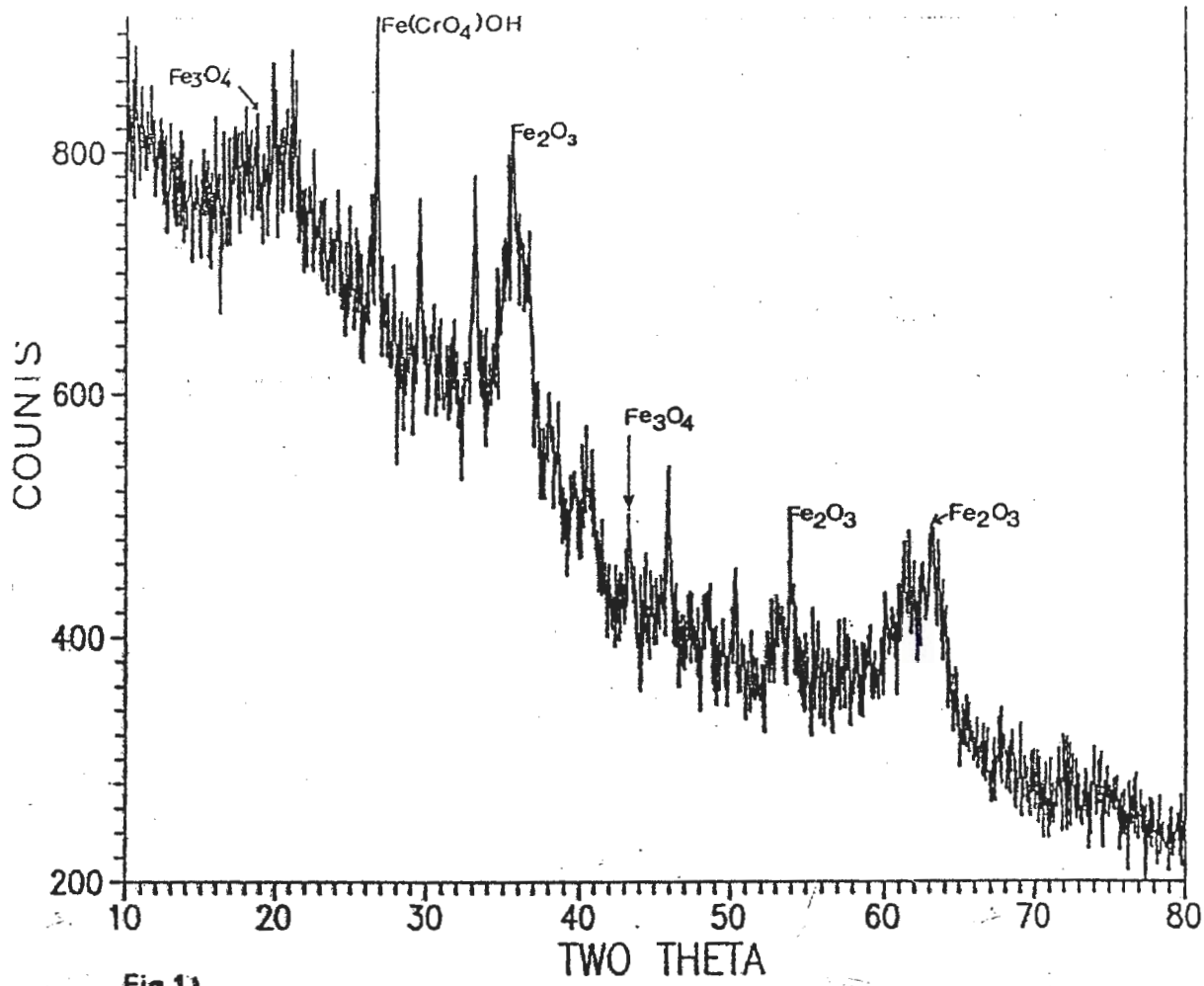


Fig 11

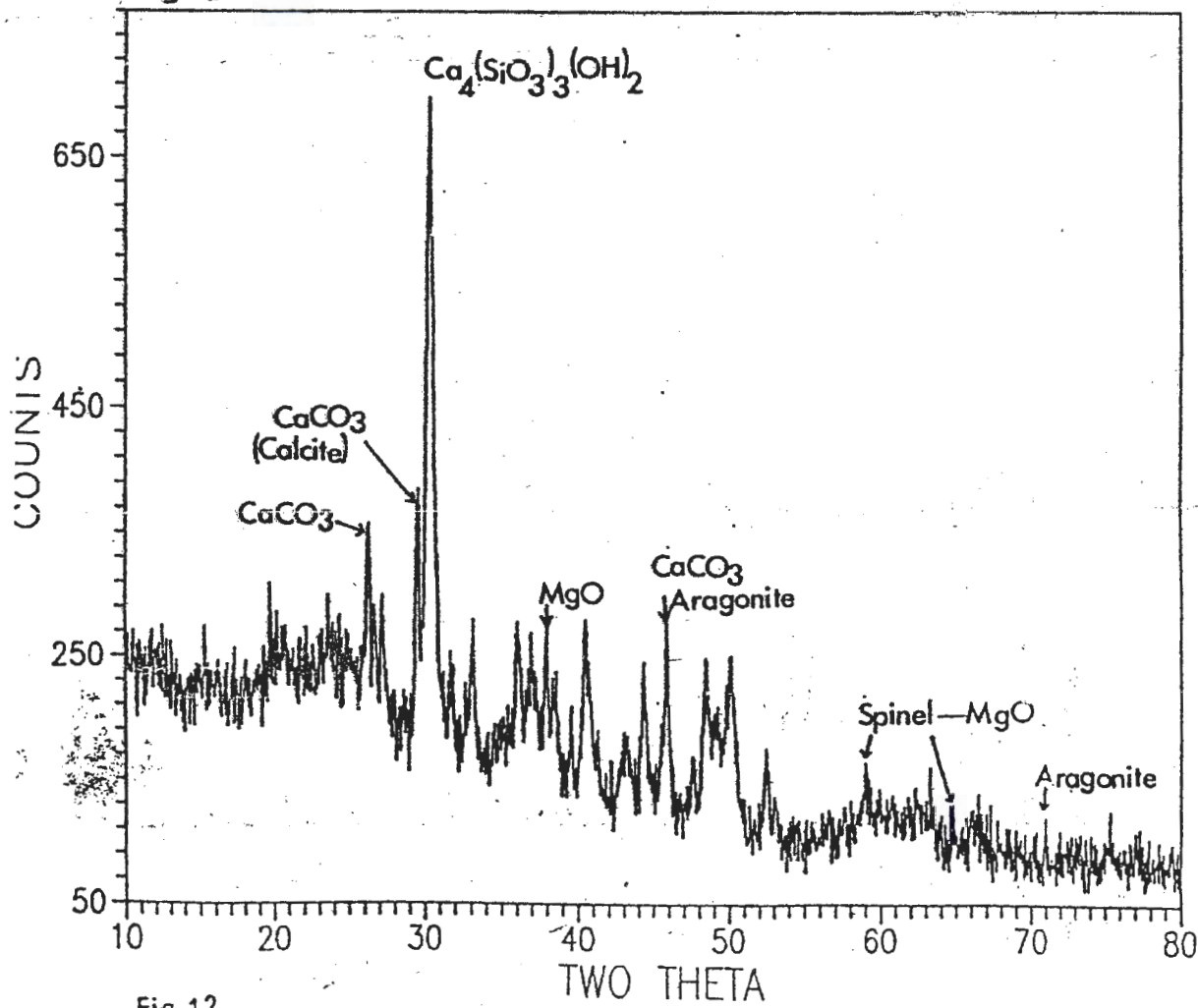


Fig 12

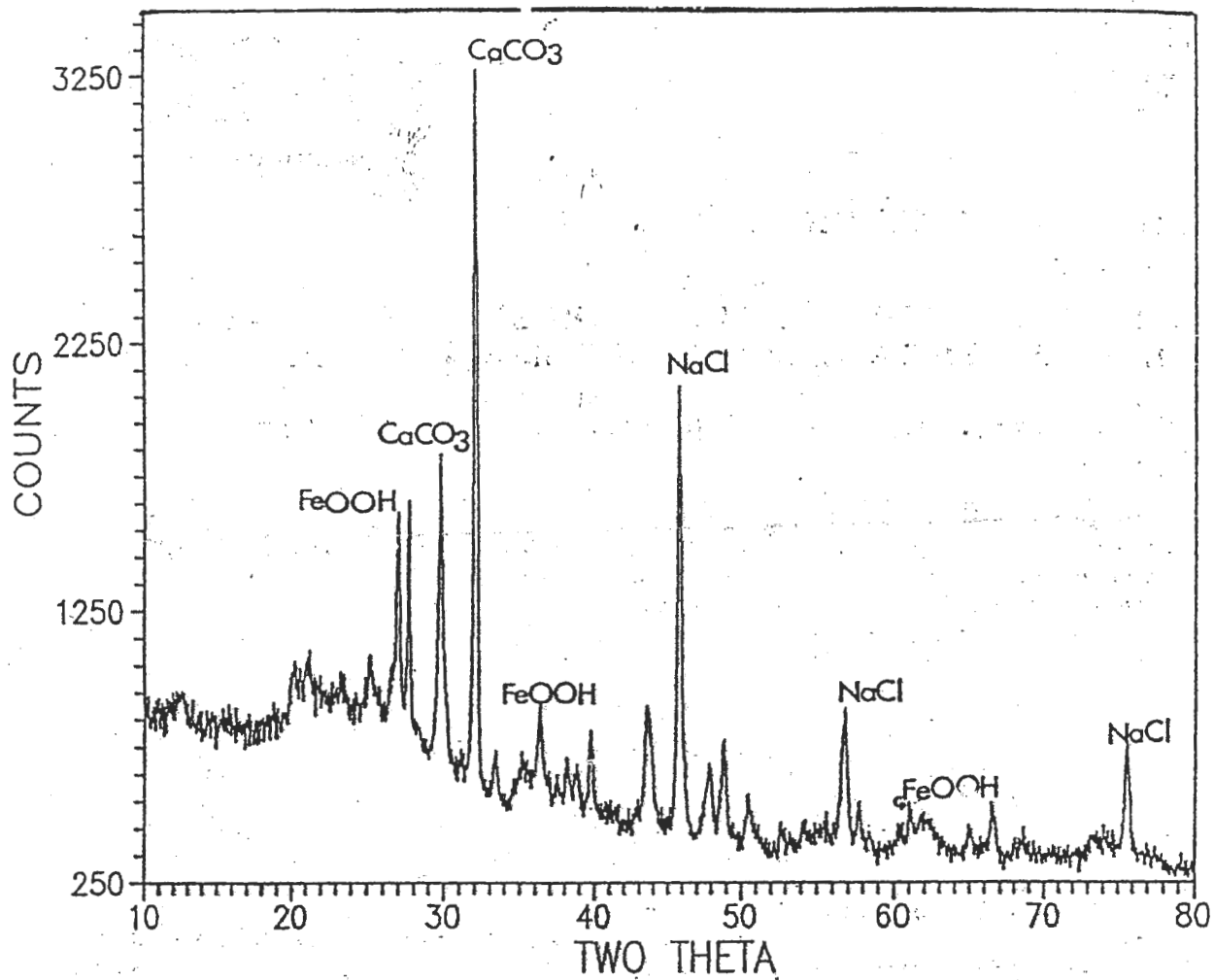


Fig.13.